A biophysical process model of tree mortality in surface fires

S.T. Michaletz and E.A. Johnson

Abstract: The mechanisms governing tree mortality in surface fires are poorly understood, owing in large part to the absence of a process-based framework for defining and evaluating these mechanisms. This paper begins the development of such a framework by deriving a first-order process model of tree mortality in surface fires (intensities less than approximately 2500 kW·m^{-1}). A buoyant line-source plume model is used to drive heat transfer models of vascular cambium and vegetative bud necroses, which are linked to tree mortality using an allometrically-based sapwood area budget. Model predictions are illustrated for white spruce (*Picea glauca*), lodgepole pine (*Pinus contorta*), and trembling aspen (*Populus tremuloides*) and are compared with independent mortality data for Engelmann spruce (*Picea engelmannii* Parry ex Engelm.) and *Pinus contorta* Dougl. Results help define first-order mortality mechanisms and suggest second-order mortality mechanisms that should be incorporated into future modeling efforts.

Résumé : Les mécanismes qui régissent la mortalité des arbres à la suite d'un feu de surface sont peu connus, surtout à cause de l'absence de cadre théorique basé sur les processus permettant de définir et d'évaluer ces mécanismes. Cet article jette les bases d'un tel cadre théorique en dérivant un modèle de premier ordre de mortalité des arbres basé sur les processus à la suite d'un feu de surface (intensité inférieure à environ 2500 kW·m^{-1}). Un modèle de panache flottant dont la source est linéaire est utilisé pour faire fonctionner des modèles de transfert de chaleur du cambium vasculaire et de nécrose des bourgeons foliaires, laquelle est reliée à la mortalité des arbres grâce à un bilan de surface d'aubier basé sur des relations allométriques. Les prédictions du modèle sont illustrées pour l'épinette blanche (*Picea glauca*), le pin tordu (*Pinus contorta*), et le peuplier faux-tremble (*Populus tremuloides*) et sont comparées à des données indépendantes de mortalité pour le l'épinette d'Engelmann (*Picea engelmannii* Parry ex Engelm.) et *Pinus contorta* Dougl. Les résultats aident à définir les mécanismes de premier ordre et à suggérer des mécanismes de second ordre à l'origine de la mortalité. Ces mécanismes devraient être retenus lors de tentatives futures de modélisation.

[Traduit par la Rédaction]

Introduction

Tree mortality in surface fires has traditionally been modeled using logistic regression, which derives a continuous probability function from binary mortality data and a suite of covariates that characterize fire behavior, fire effects, and (or) tree size (Appendix A, Table A1). While this regression approach has been useful for describing the probability of mortality within particular data sets, it has several limitations that can hinder progress towards a more mechanistic understanding. For example, this approach cannot explain why or how the covariates cause mortality. In many cases, the covariates may be correlates of mechanistic variables, so their use in regression models can confound results and obscure causal processes. This approach does not require consideration of the functional relationships between covariates, and additional covariates cannot be included into the model as the processes become better understood. Finally, the models are not general, so a different model is required for every individual situation (e.g., see Appendix A, Table A1).

An alternative process approach seeks to define and evaluate the causal mechanisms that link fire behavior and tree mortality. The mechanisms are defined in terms of heat transfer, mass transfer, and fluid mechanics models (Fay 1994; Incropera et al. 2006). The models are constructed in a modular fashion, so the functional relationships between variables are clearly defined and processes can be included or refined as they become better understood. Because the mechanisms are the same for any tree in any surface fire, the models are general but may have to be parameterized for different species, seasons, or weather conditions.

Tree mortality in surface fires is the result of several complex coupled mechanisms (Ryan and Reinhardt 1988; Parker et al. 2006). These mechanisms can be classified as first- or second-order. First-order mechanisms control "direct" fire effects like heat transfer and the resulting tissue necroses. Second-order mechanisms result from first-order mechanisms and control "indirect" fire effects like altered physiology, insect attack, and pathogenic infection. Both classes of mechanisms are poorly understood, partly because the field lacks a theoretical framework for defining and evaluating the mechanisms. Therefore, the purpose of this paper is to suggest a simple first-order process model that can provide a general framework for the development of a more complete tree mortality model. The objectives are to: (*i*) define mechanisms of vascular cambium and vegetative bud ne-

Received 14 September 2007. Accepted 15 February 2008. Published on the NRC Research Press Web site at cjfr.nrc.ca on 19 June 2008.

S.T. Michaletz[1] and E.A. Johnson. Department of Biological Sciences and Biogeoscience Institute, University of Calgary, 2500 University Drive NW, Calgary, AB T2N 1N4, Canada.

[1]Corresponding author (e-mail: sean.michaletz@ucalgary.ca).

 doi:10.1139/X08-024 © 2008 NRC Canada

Fig. 1. Schematic diagram outlining the four fundamental processes considered in the present derivation of the model. $T_1 > T_2 > T_3$. Nomenclature is as defined in Table 1.

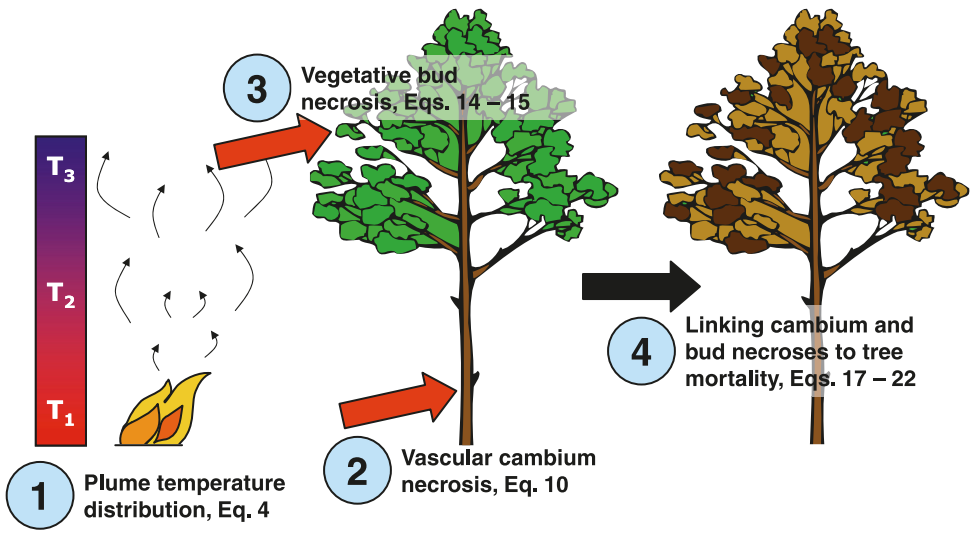

croses using physical models of surface fire plume behavior, heat transfer through bark, and heat transfer into vegetative buds; (*ii*) link vascular cambium and vegetative bud necroses to tree mortality using an allometrically-based sapwood area (SA) budget; (*iii*) illustrate model predictions for white spruce (*Picea glauca*), lodgepole pine (*Pinus contorta*), and trembling aspen (*Populus tremuloides*); and (*iv*) evaluate model predictions using independent experimental data for Englemann spruce (*Picea engelmannii* Parry ex Engelm.) and *Pinus contorta* Dougl. We would like to stress that although the cambium (Rego and Rigolot 1990) and bud (Michaletz and Johnson 2006*a*) components of the model have been validated, they have not been not been linked together and validated in the field for a whole tree. Here we evaluate the entire model using what we believe to be the best available data set (Ryan and Reinhardt 1988).

Models

We begin by considering a tree as a population of meristems (Harper 1977; White 1979). Most trees have apical and lateral meristems. Apical meristems are contained in vegetative buds and produce branches, buds, foliage, cones, and (or) flowers. Lateral meristems are contained in the vascular cambium and produce xylem and phloem vascular tissues. In a surface fire, heat transfer from the flaming fireline and plume can cause meristem necrosis by protein denaturation, which occurs at approximately 60 °C (Rosenberg et al. 1971; Dickinson and Johnson 2004). As a first approximation, tree mortality can be assumed to result from cambium necrosis around the entire circumference of the bole and (or) necrosis of all vegetative buds in the crown (Brown and DeByle 1987; Gill 1995). Necrosis of other tissues and organs (e.g., foliage, fine roots, xylem parenchyma, and (or) phloem) can alter tree physiology and contribute to mortality as well, but these second-order mechanisms are not presently considered because surviving meristems can regenerate injured tissues and organs.

Thus, the model considers four processes linking fireline combustion and tree mortality (Fig. 1): (*i*) plume buoyancy, (*ii*) conduction through the bark to the vascular cambium, (*iii*) convection to vegetative buds, and (*iv*) vascular transport processes that drive tree form. Buoyant plume theory is used to estimate the vertical plume temperature (T_p) distribution that will drive heat transfer to the vascular cambium and vegetative buds. Heat transfer theory is used to calculate the depth of vascular cambium necrosis and height of vegetative bud necrosis. Tree allometry models are then used to link cambium and bud necroses to tree mortality.

Fire T_p *distribution*

For a line-source plume in a quiescent atmosphere (no wind), the height-dependent maximum mean buoyancy, α_z, can be characterized as

$$[1] \qquad \alpha_z = C\left(\frac{1}{z}\right)\left(\frac{gI}{\rho_a c_a T_a}\right)^{2/3}$$

where C is the plume proportionality constant, z is height, g is gravitational acceleration, I is fireline intensity, ρ_a is ambient air density, c_a is the specific heat capacity of air at atmospheric pressure, and T_a is ambient temperature (cf. Raupach 1990; nomenclature defined in Table 1). α_z is a function of the temperature rise above T_a, $\Delta T_z = T_p - T_a$, where T_p is dependent on height.

$$[2] \qquad \alpha_z = \frac{g\Delta T_z}{T_a}$$

Substituting eq. 2 into eq. 1 and rearranging gives T_p as

$$[3] \qquad T_p = C\left(\frac{1}{z}\right)\left(\frac{T_a + 273.15}{g}\right)^{1/3}\left(\frac{I}{\rho_a c_p}\right)^{2/3} + T_a$$

Because this similarity analysis fails at heights comparable with the fireline width (Raupach 1990), T_p is constrained to a maximum flame temperature of 900 °C so that

$$[4] \qquad T_p = \min\left[900,\ C\left(\frac{1}{z}\right)\left(\frac{T_a + 273.15}{g}\right)^{1/3}\left(\frac{I}{\rho_a c_p}\right)^{2/3} + T_a\right]$$

This maximum flame temperature agrees with experimental

© 2008 NRC Canada

Table 1. List of symbols.

Symbol	Definition	Unit
Roman letters		
A	Wetted (convective) surface area	m^2
a	Constant parameter	na
B	Normalization constant	dimensionless
b	Constant parameter	na
C	Plume proportionality constant	Dimensionless
c	Specific heat capacity	$J \cdot kg^{-1} \cdot {}^\circ C^{-1}$
D	Diameter (outside bark)	m
d	Diameter (inside bark)	m
F	Bole taper function	na
g	Gravitational acceleration	$m \cdot s^{-2}$
h	Convection heat transfer coefficient	$W \cdot m^{-2} \cdot C^{-1}$
I	Fireline intensity	$kW \cdot m^{-1}$
k	Thermal conductivity	$W \cdot m^{-1} \cdot {}^\circ C^{-1}$
LA	Leaf area	cm^2
LCR	Live crown ratio	Dimensionless
M	Mortality number	Dimensionless
m	Mass	kg
N	Pure number	Dimensionless
n	Scaling exponent	Dimensionless
SA	Sapwood area	cm^2
T	Temperature	°C
t	Time	s
U	Plume velocity	$m \cdot s^{-1}$
V	Volume	m^3
W	Water content (proportion dry mass)	Dimensionless
X	Relative bole height	Dimensionless
x	Distance or depth	m
Z	Tree height	m
z	Height (above bole base)	m
Greek letters		
α	Maximum mean buoyancy	$m \cdot s^{-2}$
α	Thermal diffusivity	$m^2 \cdot s^{-1}$
θ	Excess temperature ratio	Dimensionless
ρ	Density	$kg \cdot m^{-3}$
Subscripts		
0.1	Basal height (z = 0.1 m)	
1.3	Breast height (z = 1.3 m)	
a	Ambient or air	
b	Bark	
ba	Basal	
bu	Bud	
c	Critical for necrosis	
d	Cured	
f	Field condition	
i	Inside bark	
lcb	Live crown base	
m	Moisture	
n	Necrosis	
p	Plume	
r	Reaction (residence)	
s	Surface	
SA	Sapwood area	
t	Total	
w	Water	
z	Height	

Note: na, not applicable.

measurements (800–1000 °C; Weber et al. 1995; Butler et al. 2004) and is well below theoretical estimates of adiabatic temperatures for forest fuels (≈ 1325 ± 100 °C; Drysdale 1999). Note that the present derivation assumes a constant top-hat temperature profile across the plume width (Mercer and Weber 2001). The relatively simple model used here was chosen to capture the most fundamental physical processes underlying T_p distributions. Readers interested in more detailed plume models that consider processes like combustion, wind, and time dependency of temperature should consult Albini (1981), Mercer and Weber (1994), and Mell et al. (2007).

Vascular cambium necrosis (bole girdling)

Vascular cambium necrosis is a one-dimensional transient conduction problem characterized by Fourier's law

$$[5] \qquad \frac{\partial^2 T}{\partial x^2} = \frac{1}{\alpha}\frac{\partial T}{\partial t}$$

where T is temperature, x is radial position (bole depth), α is thermal diffusivity of bark, and t is time (cf. Spalt and Reifsnyder 1962; Incropera et al. 2006). Solving eq. 5 using the initial condition $T(x,0) = T_a$ and boundary condition $T(0,t) = T_s$ for $t > 0$ yields

$$[6] \qquad \frac{T(x,t) - T_s}{T_a - T_s} = \mathrm{erf}\left[\frac{x}{2(\alpha t)^{1/2}}\right]$$

where $T(x,t)$ is the radial temperature distribution, T_s is the bark surface temperature, and erf is the error function. The radial bole necrosis depth, x_n, is calculated by defining $T(x,t) = T(x_n,t_r) = T_n$ and $T_s = T_p$, so that eq. 6 can be rewritten as

$$[7] \qquad \frac{T_n - T_p}{T_a - T_p} = \mathrm{erf}\left[\frac{x}{2(\alpha t)^{1/2}}\right]$$

where T_n is the meristem necrosis temperature. Note that the $T_s = T_p$ definition implicitly accounts for radiation and convection processes linking plume and bark surface temperatures. The first term in eq. 7 can be nondimensionalized by introducing the excess temperature ratio θ, which is used here as a measure of T_p relative to T_n and T_a

$$[8] \qquad \theta = \frac{T_n - T_p}{T_a - T_p}$$

Substituting eq. 8 in eq. 7 gives (Gill et al. 1986; Gutsell and Johnson 1996; Dickinson and Johnson 2004)

$$[9] \qquad \theta = \mathrm{erf}\left[\frac{x}{2(\alpha t)^{1/2}}\right]$$

which can be rearranged to give x_n as

$$[10] \qquad x_n = 2(\alpha t_r)^{1/2}\mathrm{erf}^{-1}(\theta)$$

where t_r is the fireline reaction (residence) time (Nelson 2003) and erf^{-1} is the inverse error function.

Vegetative bud necrosis (crown scorch)

Vegetative bud necrosis is characterized using a lumped capacitance analysis, which equates the rate of convection heat transfer to the bud surface with the rate of internal heat accumulation (Michaletz and Johnson 2006*a*)

$$[11] \qquad -hA(T - T_p) = \rho c_{bu} V\left(\frac{dT}{dt}\right)$$

where h is the average heat transfer coefficient, A is the

© 2008 NRC Canada

wetted (convective) surface area, T is the bud temperature, ρ is the bud mass density, c_{bu} is the specific heat capacity of the bud, V is the bud volume, and dT/dt is the rate of internal temperature change. Integrating from initial conditions $T = T_a$ at $t = 0$ and rearranging yields

$$[12] \qquad \frac{T - T_p}{T_a - T_p} = \exp\left[\left(-\frac{hA}{\rho c V}\right)t\right]$$

Defining $T = T_n$ and substituting eq. 8 in eq. 12 gives

$$[13] \qquad \theta = \exp\left[\left(-\frac{hA}{\rho c V}\right)t\right]$$

To estimate the bud necrosis height, z_n, we define $T_p = T_c$ and rearrange eq. 3 to yield (Michaletz and Johnson 2006*a*)

$$[14] \qquad z_n = C\left(\frac{1}{T_c - T_a}\right)\left(\frac{T_a + 273.15}{g}\right)^{1/3}\left(\frac{I}{\rho_a c_p}\right)^{2/3}$$

The critical T_p required for bud necrosis, T_c, is obtained by rearranging eq. 12 and defining $T_p = T_c$ and $t = t_r$, so

$$[15] \qquad T_c = \frac{T_n - \theta T_a}{1 - \theta}$$

where $\theta = \exp(-hA/\rho c V)t_r$ (eq. 13).

Linking cambium and bud necroses to tree mortality

Tree mortality is quantified by the mortality number, M, which is the proportion of necrotic buds in the crown. Whole-tree mortality ($M = 1$) can result from bole girdling and (or) complete crown scorch. Note that the interactions between partial bole girdling and partial crown scorch may also lead to mortality ($M = 1$), but this is not considered in the present derivation. When whole-tree mortality does not occur ($M \leq 1$), M expresses the proportion of crown scorch. M is thus given by

$$[16] \qquad M = \left(\frac{N_n}{N_t}\right)^{1-U(x_n/x_{ba})}$$

where N_n is the number of necrotic vegetative buds, N_t is the total number of vegetative buds in the crown, and x_{ba} is the basal bark thickness. The Heaviside step function $U(x_n/x_{ba})$ acts as a "switch" to turn bole girdling on or off:

$$[17] \qquad U\left(\frac{x_n}{x_{ba}}\right) = \begin{cases} 0 & \frac{x_n}{x_{ba}} < 1 \\ 1 & \frac{x_n}{x_{ba}} \geq 1 \end{cases}$$

When x_n (eq. 10) is greater than or equal to x_{ba}, the bole is girdled ($U(x_n/x_{ba}) = 1$) and tree mortality occurs ($M = 1$). When x_n is less than x_{ba}, the bole is not girdled ($U(x_n/x_{ba}) = 0$) and M is given by the proportion of crown scorch N_n/N_t ($M \leq 1$).

To facilitate analysis, x_{ba} and N_t from eq. 16 can be related allometrically. We build from the pipe model, which predicts tree form by assuming that a unit of leaf area (LA) is supported by a unit of cross-sectional SA (Shinozaki et al. 1964). In other words, the pipe model assumes that the Huber value (SA:LA) is constant throughout a tree, so that estimates of SA at any point along the bole can be used to calculate the distal LA. We add to this assumption the additional assumption of a constant ratio of LA to number of buds (LA:N_{bu}). Thus, by substitution, a constant ratio of SA:N_{bu} is assumed. Equation 16 can then be rewritten as

$$[18] \qquad M = \left(1 - \frac{SA_n}{SA_{lcb}}\right)^{1-U(x_n/x_{ba})}$$

where SA_n is the bole SA at z_n and SA_{lcb} is the bole SA at the height of the live crown base. SA is an appropriate framework for modeling tree form because resource distribution is considered a fundamental process driving allometric patterns (e.g., Shinozaki et al. 1964; Patterson 1992; West et al. 1999; Dreyer and Puzio 2001; Banavar et al. 2002; Niklas and Spatz 2004).

The scaling of x_{ba} with SA taper can be described using well-established allometric relationships. Bark thickness, x, scales linearly with bole diameter, D, as

$$[19] \qquad x = aD + b$$

with slope a and intercept b (Ryan and Reinhardt 1988; although for curvilinear relationships see Gill and Ashton 1968; Harmon 1984). Bole SA scales with D according to

$$[20] \qquad SA = BD^n$$

where B is a normalization constant and n is a scaling exponent (West et al. 1999). D at any height is related to the diameter at breast height $D_{1.3}$ by

$$[21] \qquad \frac{d_z}{d_{1.3}} = \left(\frac{Z - z}{Z - 1.30}\right)^{1/(\exp F)}$$

where d_z is the diameter inside bark at z, $d_{1.3}$ is the diameter inside bark at $z = 1.30$ m, and Z is tree height (Newnham 1991). The scaling exponent $1/(\exp F)$ varies continuously along Z to account for height-dependent changes in bole form (neiloidal, paraboloidal, or conical). Z scales with $D_{1.3}$ according to

$$[22] \qquad Z = B(D_{1.3}^n) + 1.3$$

(Niklas and Spatz 2004). Together, these allometric relationships can describe the scaling of x_{ba} with SA taper in boles.

Methods

Cambium x_n and critical $D_{1.3}$

x_n values are calculated (eq. 10) for *P. glauca*, *P. contorta*, and *P. tremuloides* across a range of intensities typical of surface fires. A constant $t_r = 30$ s was assumed for all calculations. This is an approximate mean for surface fires that combust fine fuels (Albini 1985; Burrows 2001), which have t_r values (Nelson 2003) of approximately 30 s (Anderson 1969; Burrows 2001; Taylor et al. 2004).

To calculate θ (eqs. 8 and 10), T_n was taken as 60 °C (Rosenberg et al. 1971; Dickinson and Johnson 2004) and T_a was taken as 25 °C. T_p was obtained from eq. 4 in which C was taken as 2.6 (Yuan and Cox 1996), z as 0.1 m, g as 9.8 m·s^{-2}, ρ_a as 1.169 kg·m^{-3} (power function fit to handbook data; Incropera et al. 2006), and c_a as 1.007 J·kg^{-1}·°C^{-1} (fifth-order polynomial fit to handbook data; Vargaftik 1975). I was varied from 0 to 2500 kW·m^{-1}. This range is

© 2008 NRC Canada

typical of surface fires and was chosen because crowning begins above approximately 2500 kW·m^{-1} (Van Wagner 1977; Johnson 1992). Given these parameter estimates, eq. 4 predicts a constant T_p of 900 °C regardless of I, an intuitive result since flame temperatures are essentially constant and flaming combustion occurs at z values of 0.1 m for $0 < I \leq$ 2500 kW·m^{-1}. Note that as a first approximation T_p was not constrained to allow for evaporation or combustion processes that may occur in bark.

Bark thermal diffusivity α is given by

$$[23] \qquad \alpha = \frac{k}{\rho c_b}$$

where k is bark thermal conductivity, ρ is bark mass density, and c_b is the specific heat capacity of the bark at constant pressure. k was calculated as (Martin 1963)

$$[24] \qquad k = (2.104\rho_b + 5.544\rho_m + 3.266T - 166.216) \times 10^{-4}$$

with T = 25 °C. ρ_b is given by

$$[25] \qquad \rho_b = \frac{m_d}{V_f}$$

where m_d is the cured mass (oven-dried at 90 °C to a constant mass) and V_f is the volume at field water content. ρ_b values were taken as 453.32 kg·m^{-3} for *P. glauca*, 536.62 kg·m^{-3} for *P. contorta*, and 578.27 kg·m^{-3} for *P. tremuloides* (Millikin 1955). The moisture density, ρ_m, is given by

$$[26] \qquad \rho_m = (W + W^2)\rho_b$$

Water content, W (proportion dry mass), was calculated as

$$[27] \qquad W = \frac{m_f - m_d}{m_d}$$

where m_f is the mass at field water content. Bark water content during a fire event will generally be lower than the seasonal mean because bark and fine fuel water contents are controlled by the same processes (Viney 1991; Matthews 2006). However, in the absence of the meteorological data required to calculate fine fuel moisture (Matthews 2006), W values were calculated using bark samples collected at the Kananaskis Field Stations in the southern Rocky Mountains of Alberta, Canada. Samples were collected weekly from 18 May to 5 October 2004 (7 samples per species per week; 140 samples per species in total). W values ($W_{P.\ glauca}$ = 0.889; $W_{P.\ contorta}$ = 0.591; $W_{P.\ tremuloides}$ = 0.701) were then used to calculate ρ_m values of 761.27 kg·m^{-3} for *P. glauca*, 504.57 kg·m^{-3} for *P. contorta*, and 689.53 kg·m^{-3} for *P. tremuloides*. c_b was calculated as

$$[28] \qquad c_b = 1105.315 + 4.857T + Wc_w + 348.342$$

where the specific heat capacity of water, c_w, is 4180 J·kg^{-1}·°C^{-1} and T is 25 °C (Martin 1963).

$x_n$values were used to estimate the critical $D_{1.3}$ for each species. The basal diameter, $D_{0.1}$, was first estimated by defining $x_n = x_{ba}$ and using eq. 19, where constants a and b are tabulated in Table B1 (calculated from Huang 1994). Critical $D_{1.3}$ was then estimated from $D_{0.1}$ using eq. 21 (F functions are tabulated in Table B2; Newnham 1991) with eq. 19 (Table B1) and eq. 22 (constants B and n are tabulated in Table B3; Peng 1999).

z_n and vertical bud distributions

First, z_n is calculated for *P. glauca*, *P. contorta*, and *P. tremuloides*, then SA taper is used to estimate vertical bud distributions and proportion of bud necrosis. z_n is estimated using eq. 14 with the plume parameter values used above for cambium x_n. T_c values were calculated using eq. 15, in which T_n = 60 °C (Rosenberg et al. 1971; Dickinson and Johnson 2004) and θ was calculated using eq. 13 with inverse thermal time constant, $hA/\rho cV$, values from Table B4 (Michaletz and Johnson 2006*a*). $hA/\rho cV$ values were obtained from *P. glauca* and *P. contorta* or calculated using methods of Michaletz and Johnson (2006*a*) for *P. tremuloides*. The values used are means calculated over the entire fire season and in different canopy positions (i.e., low and high light regimes). Heat transfer coefficients, h, were calculated using convection correlations for foliated conifer buds (*P. glauca* and *P. contorta*; Michaletz and Johnson 2006*b*) and cylinders (corresponding to the leafless or dormant stage; *P. tremuloides*; Hilpert 1933), assuming a constant plume velocity of U = 5.0 m·s^{-1}. Leafless *P. tremuloides* were used here because convection correlations are not available for buds shielded by broadleaves; note that the model is still applicable to broadleaf species in the foliated stage, provided appropriate convection correlations are used.

Vertical bud distributions were calculated from SA taper. SA taper is an effect of branching and thus reflects crown form. SA taper can be expressed as a cumulative survival distribution

$$[29] \qquad S(z) = \frac{\mathrm{SA}_z}{\mathrm{SA}_{\mathrm{lcb}}}$$

Here, SA_z is the SA at z and $\mathrm{SA}_{\mathrm{lcb}}$ is the SA at height of live crown base, z_{lcb}, which is given by

$$[30] \qquad z_{\mathrm{lcb}} = Z - Z(\mathrm{LCR})$$

To estimate z_{lcb}, mean (± SEM) live crown ratio (LCR) values were calculated from BOREAS data sets (*P. glauca* 0.85 ± 0.07, N = 8; *P. banksiana* 0.62 ± 0.02, N = 163; *P. tremuloides* 0.34 ± 0.01, N = 210; Gower and Vogel 1997; Rich and Fournier 1997). To obtain SA values, SA_z and $\mathrm{SA}_{\mathrm{lcb}}$ in eq. 29, eq. 21 was rearranged to give inside diameter, d_z, as

$$[31] \qquad d_z = D_i\left(\frac{Z - z}{Z - 1.30}\right)^{1/\exp F}$$

where F functions are tabulated in Table B3 (Newnham 1991). d_z was then used to estimate outside diameter, D_z, by rearranging eq. 19 so that

$$[32] \qquad D_z = \frac{d_z + 2b}{1 - 2a}$$

where constants a and b are tabulated in Table B1 (calculated from Huang 1994). SA_z and $\mathrm{SA}_{\mathrm{lcb}}$ were then calculated from D_z and D_{lcb} using eq. 20, where B and n values (Table B5) were estimated by Model II reduced major axis regression (Sokal and Rohlf 1995) on log-transformed bole dia-

© 2008 NRC Canada

meter and SA data (obtained from R.J. Hall; Hall et al. 2003). Analyses were performed using (S)MATR computer software (Falster et al. 2003).

Assuming a constant SA:N_b ratio (see Models section above) and horizontal branching, the vertical bud distribution N_b/N_{total} is given by the cumulative mortality distribution

$$[33] \quad \begin{aligned} F(z) &= 1 - S(z) \\ &= 1 - \frac{SA_z}{SA_{lcb}} \\ &= \frac{N_b}{N_{total}} \end{aligned}$$

Tree mortality predictions

Tree mortality is estimated using eq. 18, which links vascular cambium necrosis (bole girdling) with vegetative bud necrosis (crown scorch proportion). Results are plotted as mortality surfaces, which relate $D_{1.3}$, I, and the proportion of necrotic vegetative buds, M.

Vascular cambium necrosis is estimated by comparing radial x_n with x_{ba}. For a given $D_{1.3}$, x_{ba} was estimated using eqs. 19, 21, 22, and 32 with parameter estimates from Tables B1, B2, and B3. x_n was calculated using eq. 10 with the same plume and bark parameter values used above for calculating cambium necrosis and critical $D_{1.3}$. Simulations were then conducted for t_r values of 10, 20, 30, 40, 50, and 60 s.

The proportion of vegetative bud necrosis (crown scorch) is estimated by comparing the bole SA at z_n, SA_n, with the bole SA at crown base height, SA_{lcb}. SA_n is estimated by first defining z as z_n (eq. 21) to give the diameter inside bark at necrosis height, d_n. Equation 32 is then used to estimate outside diameter at necrosis height, D_n, and finally eq. 20 is used to estimate SA_n. SA_{lcb} is estimated in the same manner, after defining z as z_{lcb} (eq. 30).

Model evaluation

A rigorous statistical validation requires the measurement of T_a (eqs. 4 and 10), bark water content (to calculate α in eq. 10), I (eq. 3), t_r (eq. 10), bud $hA/\rho cV$ (eq. 14), bark thickness allometry (eq. 19), SA allometry (eq. 20), bole taper (eq. 21), Z (eq. 22), z_{lcb} (eq. 30), and M (proportion of necrotic buds). To minimize the confounding effects of second-order mortality mechanisms, mortality should be censused as soon as possible following the fire event. Unfortunately, we are not aware of any data sets that contain all of these required variables (see Appendix A, Table A1). Furthermore, because investigators are generally concerned with long-term effects, mortality is typically censused up to several years following the fire event.

Given the lack of suitable data for statistical validation, we evaluated the model using a weaker test that compared predictions for *P. glauca* and *P. contorta* with surface fire mortality data for *P. engelmannii* and *P. contorta* (obtained from K.C. Ryan; Ryan and Reinhardt 1988). Data were not available for *P. tremuloides*. For each tree, available data included $D_{1.3}$, foliage necrosis height (visual estimate), foliage necrosis proportion (visual estimate), and postfire status (alive or dead; *P. engelmannii* censused for 3 years postfire, and *P. contorta* censused up to 8 years postfire). Model predictions were based on the plume and tree parameter estimates described above for tree mortality predictions because site- and species-specific parameter estimates were not available. A t_r value of 30 s was assumed, which is an approximate mean value for surface fires (Anderson 1969; Burrows 2001; Taylor et al. 2004). I was estimated from foliage necrosis height (Van Wagner 1973) because variables required for calculation (linear spread rate and combusted fuel mass per unit area) or correlation (flame length) were not available. M was taken as 1 for trees with "dead" status and as the proportion of foliage necrosis for trees with "alive" status (M was not available). Note that mortality was censused several years following the fire events, so observed values of M are confounded by second-order mortality mechanisms that are not currently considered by the model. Mortality data were then plotted with model predictions for $0 < I \leq 2500$ kW·m^{-1}.

Table 2. x_n (cm) and critical $D_{1.3}$ (cm) for *Picea glauca*, *Pinus contorta*, and *Populus tremuloides* boles.

Species	x_n (cm)	Critical $D_{1.3}$ (cm)
P. glauca	0.733	34.982
P. contorta	0.670	30.650
P. tremuloides	0.694	18.039

Note: x_n calculated using α for bark and assuming t_r = 30 s. Critical $D_{1.3}$ calculated assuming $x_n = x_{ba}$. Nomenclature is as defined in Table 1.

Results

Cambium x_n and critical $D_{1.3}$

Cambium x_n values and corresponding critical $D_{1.3}$ values for $0 < I \leq 2500$ kW·m^{-1} are shown in Table 2. For each species, x_n and critical $D_{1.3}$ are constant with I because T_p is 900 °C at z = 0.1 m. x_n is greatest for *P. glauca*, followed by *P. tremuloides* and *P. contorta*, but because of differences in bark thickness relationships (Table B1) and bole taper exponents (Table B2), the critical $D_{1.3}$ is largest for *P. glauca*, followed by *P. contorta* and *P. tremuloides*.

z_n and vertical bud distributions

z_n is greatest for *P. tremuloides*, followed by *P. glauca* and *P. contorta* (Fig. 2). *Populus tremuloides* has the highest z_n because it has relatively small buds that are not shielded by foliage, resulting in a relatively large $hA/\rho cV$ value (low T_c; Table B4). *Pinus contorta* has the lowest z_n because it has relatively large buds that are shielded by long, densely packed foliage (Michaletz and Johnson 2006*b*), resulting in a relatively small $hA/\rho cV$ value (high T_c; Table B4). Power function fits to predicted data (*P. glauca*, $z_n = 0.100\ I^{2/3}$; *P. contorta*, $z_n = 0.073\ I^{2/3}$; *P. tremuloides*, $z_n = 0.183\ I^{2/3}$) reflect the 2/3 power scaling of T_p with I from eq. 14 (Van Wagner 1973; Michaletz and Johnson 2006*a*).

For a given z_n, the proportion of bud necrosis can be estimated using cumulative vertical bud distributions derived from SA budgets (Fig. 3). Taper exponents are also plotted in Fig. 3. Recall that the vertical bud distribution, N_b/N_{total} =

© 2008 NRC Canada

Fig. 2. Vegetative bud necrosis heights for *Picea glauca* (foliated), *Pinus contorta* (foliated), and *Populus tremuloides* (leafless), assuming an ambient temperature (T_a) of 25 °C.

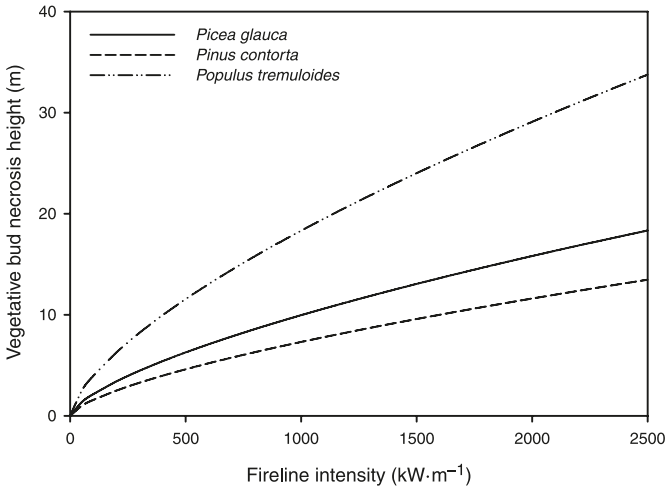

$1 - (SA_z/SA_{lcb})$. Results are plotted over normalized height $(z - z_{lcb})/(Z - z_{lcb})$ to allow comparison between species and size classes. For *P. glauca*, SA taper and vertical bud distributions vary with height. The highest taper exponents are found at the bottom of the crown, indicating that the bottom has more buds per height increment than the top (considering only apical meristems at the ends of branches and not epicormic buds on the bole). SA taper and vertical bud distributions also vary with tree size ($D_{1.3}$), changing from approximate linear functions (SA taper exponent $n_{SA}/\exp F \approx 1$) to nearly quadratic ($n_{SA}/\exp F \approx 2$) as size increases. This indicates that as a tree grows in size, proportionally more buds are found in the bottom of the crown as compared with smaller trees. Similar results are observed for *P. contorta*, although the highest taper exponents are generally found at the top of the crown, which has more buds per height increment than the bottom. SA taper and vertical bud distributions also vary with size, changing from approximately linear ($n_{SA}/\exp F \approx 1$) to borderline linear and (or) quadratic ($n_{SA}/\exp F \approx 1.6$) as size increases. Thus, as a tree grows in size, proportionately more buds are found in the bottom of the crown as compared with smaller trees. For *P. tremuloides*, SA taper and vertical bud distributions are nearly quadratic (SA taper exponent $n_{SA}/\exp F \approx 2$) so that crown bottoms contain more buds per increment than crown tops. This trend is consistent across all size classes, indicating consistency in crown form throughout ontogeny.

Vertical bud distributions are also plotted over absolute height (Fig. 3) to illustrate differences among species and size classes and also to facilitate estimates of proportion of vegetative bud necrosis. Here, x-intercepts correspond to z_{lcb} and $N_b/N_{total} = 1$ indicates the crown top Z. As expected on the basis of the LCR values (eq. 30), *P. tremuloides* always has the greatest z_{lcb} value, followed by *P. contorta* and *P. glauca*. *Picea glauca* has the longest total crown length, whereas *P. tremuloides* has the shortest. Height trends are less consistent, as expected on the basis of height scaling constants (Table B3). The cumulative bud distribution plotted on absolute height also provides a convenient method for estimating the proportion of bud necrosis (crown scorch). The proportion of vegetative bud necrosis can be easily estimated from Fig. 3 by finding z_n (eq. 14; Fig. 2) on the horizontal axis and constructing a vertical line that intersects the cumulative bud distribution. The value on the vertical axis that corresponds to this intersection will give the proportion of bud necrosis.

Tree mortality predictions

Predictions for *P. glauca*, *P. contorta*, and *P. tremuloides* are plotted as mortality surfaces in Fig. 4. Surface discontinuities (from $M = 1$ to $M < 1$) reflect the Heaviside step transition from bole girdle mortality to crown scorch. Bole girdling was the primary mechanism of tree mortality for all species. Within a species, the critical $D_{1.3}$ is constant for these I values (Table 2) because $T_p = 900$ °C at $z = 1$ for all intensities (eq. 4). For given I and t_r values, *P. glauca* and *P. contorta* have larger critical $D_{1.3}$ values than *P. tremuloides*, as expected on the basis of x scaling and bole taper (Tables B1 and B2; Table 2).

As $D_{1.3}$ increases (Table 2), x_{ba} increases until it is thick enough to prevent vascular cambium necrosis (this occurs at the critical $D_{1.3}$; Table 2). Beyond this critical $D_{1.3}$, M is given by the proportion of bud necrosis (crown scorch). Bud necrosis only resulted in tree mortality ($M = 1$) for leafless *P. tremuloides* with relatively small $D_{1.3}$ values (and low height) at relatively higher surface fire intensities ($I \geq 1500$ kW·m^{-1}). The $D_{1.3}$ of leafless *P. tremuloides* that are killed by crown scorch increases with t_r, so that for high intensities at $t_r \geq 20$ s, $D_{1.3}$ for *P. tremuloides* may actually be larger than $D_{1.3}$ for *P. glauca* and *P. contorta*.

Along $D_{1.3}$ isolines, vertical bud distributions are constant, but I varies, so variation in M results from variation in z_n (Fig. 2) combined with slopes of cumulative vertical bud distributions *within* $D_{1.3}$ classes (Fig. 3). Along I isolines, z_n is constant but cumulative bud distributions vary, so variation in M is a sole result of variation in cumulative bud distributions *among* $D_{1.3}$ classes.

For *P. contorta*, M does not vary along $D_{1.3}$ isolines (Fig. 4) because bole girdling always occurs before vegetative bud necrosis. This is due to the relatively high heat resistance of buds (Table B3), relatively low z_n values (Fig. 2), and thin bark that permits vascular cambium necrosis (Table B1). *Pinus contorta* also has a LCR that elevates buds above the forest floor and lethal T_p values (Fig. 3). Variation in M is observed along I isolines (Fig. 4), and this variation reflects the Heaviside step transition from vascular cambium necrosis (bole girdling). These critical $D_{1.3}$ values increase with t_r (Fig. 4).

For *P. glauca*, M varies along $D_{1.3}$ isolines (Fig. 4) because vegetative bud necrosis occurs in almost all $D_{1.3}$ classes in all fires, with the exception of very large trees at low I values. Vegetative bud necrosis occurs because relative to *P. contorta*, *P. glauca* has less heat resistant buds (Table B3) and a larger LCR so that buds are lower to the ground and closer to lethal T_p values (Fig. 3). Variation in M is also observed along I isolines (Fig. 4), reflecting both variation in cumulative bud distributions among tree size classes (Fig. 3) as well as the Heaviside transition from cambium necrosis to crown scorch. Critical $D_{1.3}$ values and proportion of bud necrosis increase with t_r (Fig. 4).

In *P. tremuloides*, both $D_{1.3}$ and I have strong effects on

© 2008 NRC Canada

Fig. 3. Taper exponents, SA taper, and vertical bud distribution for the live crown portion of boles ($z_{lcb} \leq z \leq Z$) across a range of size classes ($5.0 \leq D_{1.3} \leq 100.0$ cm). In the first three columns, normalized height $(z - z_{lcb})/(Z - z_{lcb}) = 0$ corresponds to the crown bottom and $(z - z_{lcb})/(Z - z_{lcb}) = 1$ corresponds to the crown top. Top row, *Picea glauca*; middle row, *Pinus contorta*; bottom row, *Populus tremuloides*. Nomenclature is as defined in Table 1.

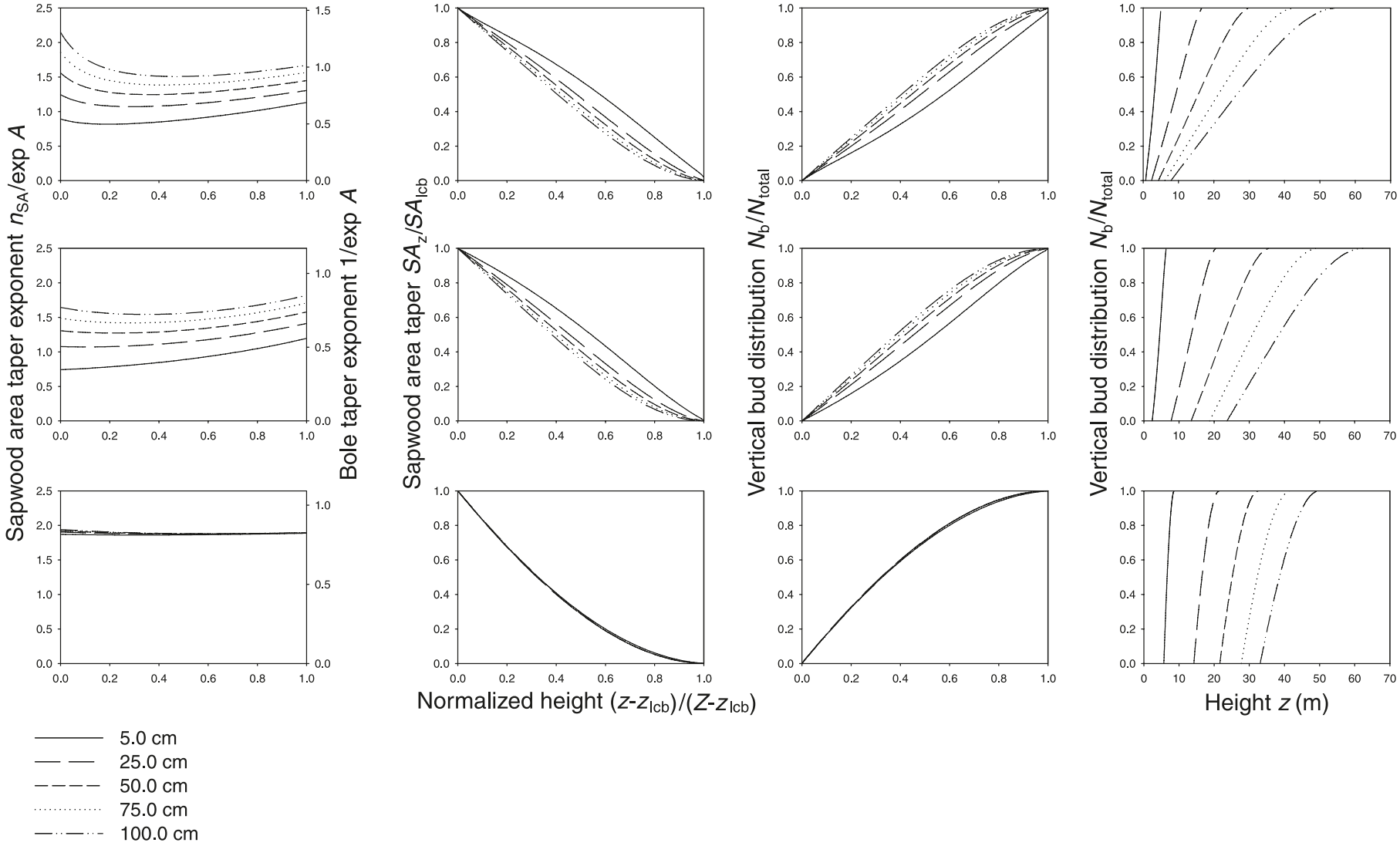

© 2008 NRC Canada

Fig. 4. Mortality surfaces for *Picea glauca*, *Pinus contorta*, and *Populus tremuloides* ($10 \leq t_r \leq 60$ s) and experimental mortality data (●) for *Picea engelmannii* and *Pinus contorta*. Surface discontinuities reflect the Heaviside transition from bole girdling to vegetative bud necrosis. M, proportion of necrotic buds; $D_{1.3}$, diameter at breast height (cm); I, fireline intensity (kW·m^{-1}). Nomenclature is as defined in Table 1.

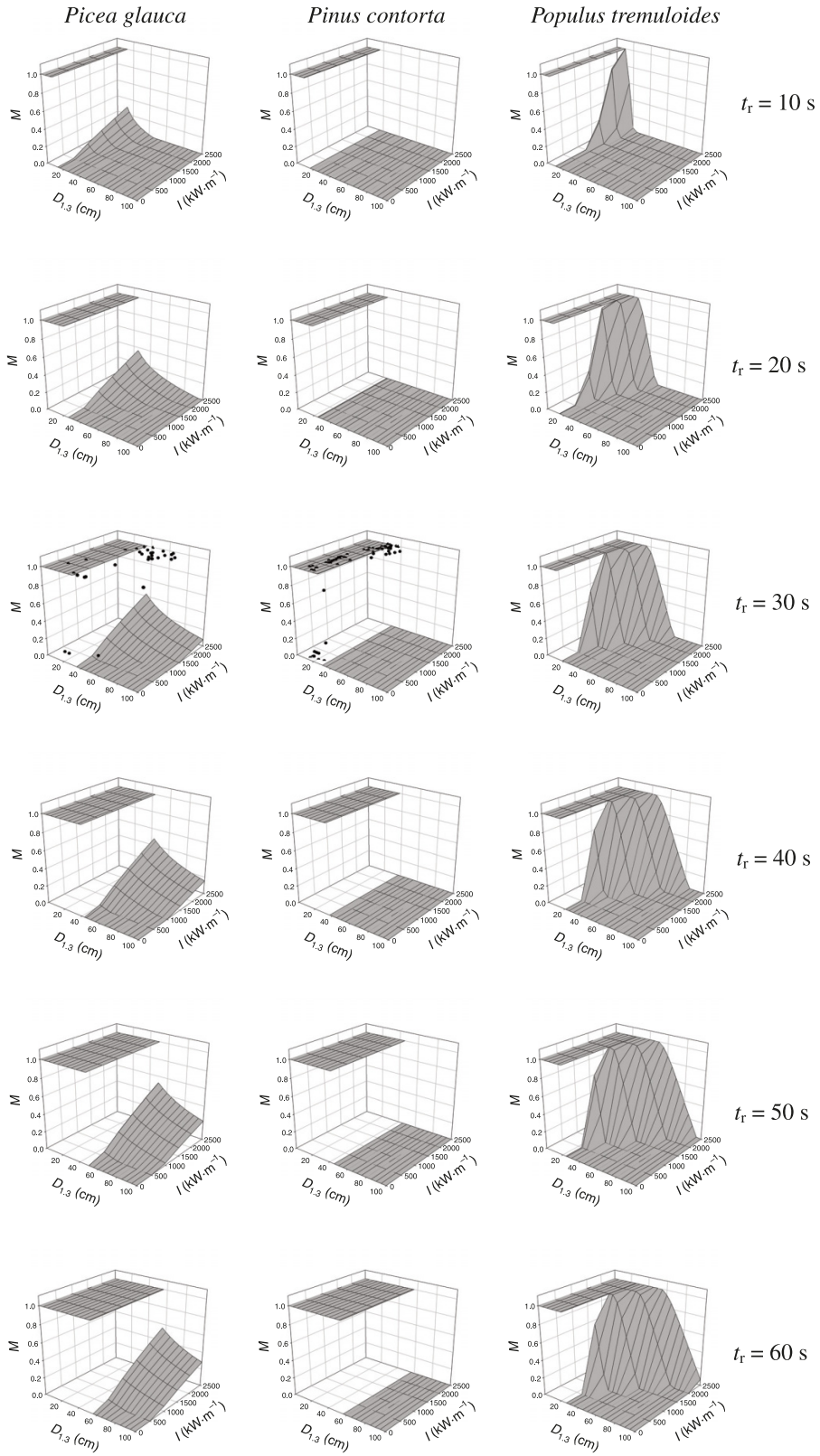

© 2008 NRC Canada

M, as demonstrated by steep slopes along I and $D_{1.3}$ isolines (Fig. 4). Variation along $D_{1.3}$ isolines is because of high rates of change with height in vertical bud distribution within a $D_{1.3}$ class, whereas variation along I isolines is because of differences in the cumulative vertical bud distribution among $D_{1.3}$ groups (Fig. 3). These differences mean that a slight increase in z_n represents a large proportional change in bud distribution and, thus, a large change in M. Critical $D_{1.3}$ values and proportion of bud necrosis increase with t_r (Fig. 4).

Model evaluation

Experimental mortality data for *P. engelmannii* and *P. contorta* are plotted with mortality surfaces for *P. glauca* and *P. contorta* (Fig. 4). For *P. glauca* and *P. engelmannii*, there is good agreement at lower $D_{1.3}$, with the exception of two points ($D_{1.3}$ < 20 cm and I < 500 kW·m^{-1}), which had much lower M than expected. However, for $D_{1.3}$ larger than the critical $D_{1.3}$ (Table 2), M was much higher than expected. In many cases, $M = 1$ and the entire tree was dead although the model predicted roughly $0.3 \leq M \leq 0.5$. Similar results were observed for *P. contorta*. At lower $D_{1.3}$ there was good agreement between predictions and observations, although there were several points for small $D_{1.3}$ and low intensities where M was much lower than predicted. There were also several points ($D_{1.3}$ slightly larger than critical for I > 1500 kW·m^{-1}) where $M = 1$ but the model predicted $M = 0$.

Discussion

This paper derives a first-order process model of tree mortality in surface fires. The present derivation is by no means a comprehensive model, but it offers insights into causal mechanisms that cannot be achieved with traditional logistic regression models. It also highlights a need within the field for data required to test models of this type. Here we discuss examples of how the model can provide insight into causal mechanisms and how this process-based framework can be extended in future modeling studies.

One issue that the process model can provide insight into is evaluation of the relative roles of bole and crown injuries in tree mortality. Results of regression analyses generally suggest that there is no good rule of thumb. For example, several studies on Douglas-fir (*Pseudotsuga menziesii* (Mirb.) Franco) have shown that crown injury is more important (Peterson and Arbaugh 1986; Wyant et al. 1986; Peterson and Arbaugh 1989), but others have shown that bole injury is more important (Ryan et al. 1988). The process model suggests that the differences between studies result from differences in fire behavior, thermophysical properties of bark and buds, or allometry. The process model has not been parameterized for *P. menziesii*, but for *P. glauca*, *P. contorta*, and leafless *P. tremuloides*; the model predicts that cambium necrosis is more important than bud necrosis for mortality (Fig. 4). However, it is important to note that at higher fireline intensities ($I \geq$ 1500 kW·m^{-1}), vegetative bud necrosis caused mortality in some *P. tremuloides* on which the bole was not girdled (Fig. 4). This shift in the relative roles of bole and crown injuries on *P. tremuloides* mortality has also been observed experimentally (Brown and DeByle 1987); in high "severity" fires immediate mortality occurred (attributed to crown scorch), whereas in low and moderate "severity" fires mortality occurred over 2 years following the fire event (attributed to bole girdling). Thus, the relative roles of bole and crown injury in tree mortality are not static, and the process model identifies causal variables that should be considered when evaluating the roles.

The process model can also help provide a better basis for ranking resistance (tolerance) of trees to fires. Fire resistance rankings are typically sketchy at best because (*i*) fire resistance lacks a consistent definition, (*ii*) fire effects vary seasonally owing to weather conditions and phenological stage, and (*iii*) it is difficult to obtain equivalent fire behavior characteristics across species. Hence, rankings have traditionally been based on qualitative morphological characteristics thought to influence mortality in fires, such as bark thickness, crown and root form, epiphyte density, and tree density (Starker 1934; Brown and Davis 1973; Minore 1979). Based on these considerations, it has generally been concluded that *P. tremuloides* and *P. glauca* have low fire resistance, whereas *P. contorta* has moderate fire resistance (although the relative rankings have been noted to vary geographically). More recent data from a passive crown fire suggest that *P. tremuloides* is less fire resistant than *P. mariana* and *P. banksiana*, which are equally resistant (Hély et al. 2003).

Ostensibly, these rankings appear to agree with process model predictions (Fig. 4). For relatively high fireline intensities ($I \approx$ 2500 kW·m^{-1}, e.g., a passive crown fire), leafless *P. tremuloides* is less resistant than *P. glauca* and *P. contorta*, which are relatively equally resistant (Fig. 4, Table 2). However, the ranking changes at low fireline intensities, where *P. tremuloides* is the most fire resistant, followed by *P. contorta* and *P. glauca*. Why do fire resistance rankings vary with I? At higher intensities, *P. tremuloides* is less resistant because although it has the lowest critical $D_{1.3}$ (most resistance to bole girdling; Table 2) it also has small, leafless buds that provide little resistance to heat transfer (Table B3). These higher intensities result in a z_n value that is greater than Z, which causes necrosis of all of the buds in the crown (Figs. 2, 3, and 4). At lower intensities, z_n is not great enough to kill all of the buds in the crown, and *P. tremuloides* has thicker bark than *P. glauca* and *P. contorta*, resulting in a larger $D_{1.3}$. Thus, fire resistance rankings vary with fire behavior characteristics. Other confounding variables include tree size and allometry, thermophysical properties of bark and buds, phenological stage, and weather conditions, and such variables should be carefully considered in fire resistance rankings.

Although the individual processes that compose the model (Fig. 1) have been validated (Rego and Rigolot 1990; Yuan and Cox 1996; Michaletz and Johnson 2006*a*), it is difficult to validate the entire mortality model because the required parameter estimates and mortality data are unavailable. To predict observed mortality data, the model requires parameter estimates for T_a, I, t_r, bark water content, bark thickness, bole taper, SA, Z, LCR, and $hA/\rho cV$ of buds. Mortality (proportion of necrotic buds) must also be censused as soon as possible following the fire event to minimize the confounding effects of second-order mortality mechanisms. Most studies have been interested in predicting long-term

© 2008 NRC Canada

mortality; therefore, censuses have typically occurred several years following the fire event. Data censused in this way reflect a combination of first- and second-order mortality mechanisms, so it is impossible to distinguish the relative roles of the various mechanisms in causing mortality. This is apparent when process model predictions are compared with long-term morality data for *P. engelmannii* and *P. contorta* (Fig. 4; Ryan and Reinhardt 1988). However, differences between predicted and observed values suggest processes that should be eventually incorporated into this process-based framework.

Fortunately, the modular construction of the process model permits inclusion or refinement of processes as they become better understood. The most obvious processes that contribute to the differences between predictions and data (Fig. 4) are altered carbon and water source-sink dynamics, which result from combined heat effects on foliage, roots, phloem, and (or) xylem. The process model presented in this paper was derived with the intention of eventually incorporating these processes. Incorporating the first-order processes should be relatively straightforward. Foliage necrosis can be modeled by a lumped capacitance analysis (Michaletz and Johnson 2006*a*, 2006*b*) and incorporated into the tree mortality model using foliage distributions obtained from Huber value estimates (Fig. 3). Likewise, fine root necrosis can be modeled using a lumped capacitance analysis linked with an existing model of heat and mass transfer through soil (e.g., Campbell et al. 1995). Necrosis of phloem and xylem ray parenchyma cells can be modeled using two-dimensional models of heat transfer in tree boles (Jones et al. 2004). However, predicting the second-order processes governing carbon and water budgets is a more complex problem that will require consideration of tree physiology processes.

The process model currently assumes that complete cambium necrosis occurs around the circumference of the bole. However, partial cambium necrosis is clearly common in low intensity surface fires, and fire scars are a good example of this (Gutsell and Johnson 1996). Partial cambium necrosis can result from differences in bark thickness (e.g., plates vs. fissures) as well as circumferential variation in bole surface temperatures (Tunstall et al. 1976; Gutsell and Johnson 1996). Although modeling variable heat transfer and cambium necrosis around the bole is straightforward, the effect of partial bole girdling on tree mortality is poorly understood. The small number of studies that have considered partial girdling by heat have found from little to no effect on mortality, although partial girdling did induce various physiological responses (Ducrey et al. 1996; Alonso et al. 2002). How partial bole girdling interacts with root and foliage necroses to alter tree physiology remains unclear.

The present derivation of the model doesn't consider smoldering combustion of duff or its effects on the roots and bole. Smoldering is a combustion process that occurs without a flame and produces heat from slow oxidation of pyrolyzed fuel elements (Miyanishi 2001). Smoldering combustion generally occurs after the passage of the flaming fireline and consequently is not directly related to I (Hartford and Frandsen 1992; Miyanishi 2001). Smoldering combustion may be particularly important for mortality of species such as *P. ponderosa*, where it is thought that nearly 100 years of fire exclusion has resulted in abnormally deep layers of duff around large boles (Ryan and Frandsen 1991; Swezy and Agee 1991). These deep layers of duff can support smoldering combustion for hours or days following passage of the flaming fireline, which can combust any fine roots located within the duff (Swezy and Agee 1991) and also conduct heat through soil and into the tree, where phloem and cambium necrosis can occur (Ryan and Frandsen 1991). Including processes of smoldering combustion into the model will first require development of a model for smoldering combustion of duff. To our knowledge, a process-model of smoldering combustion of duff has not been published, although models for packed cellulosic materials (reviewed in Miyanishi 2001) should provide insight.

Clearly, the present derivation does not consider all of the mechanisms linking fire behavior and tree mortality, because our understanding of these mechanisms is limited by the lack of process-based framework for defining and validating potential mechanisms. Progress in this area will require moving from a reliance on logistic regression models towards general process-based models. This model provides the framework for this endeavor.

Acknowledgements

The authors thank K.C. Ryan and S.M. Hood for providing mortality data used in model evaluation and for helping us to confirm that no other data sets were available. R.J. Hall kindly provided the bole diameter and SA data used to fit eq. 20. Comments from K. Miyanishi, J.J. Choczynska, and four anonymous referees improved the manuscript. This work was supported by an Alberta Ingenuity Studentship and an Alberta Conservation Association Grant in Biodiversity (to the first author) and an NSERC operating grant and the G8 Legacy Chair in Wildlife Ecology (to the second author).

References

Albini, F.A. 1981. A model for the wind-blown flame from a line fire. Combust. Flame, **43**: 155–174. doi:10.1016/0010-2180(81)90014-6.

Albini, F.A. 1985. A model for fire spread in wildland fuels by radiation. Combust. Sci. Tech. **42**: 229–258. doi:10.1080/00102208508960381.

Alonso, M., Rozados, M.J., Vega, J.A., Pérez-Gorostiaga, P., Cuiñas, P., Fontúrbel, M.T., and Fernández, C. 2002. Biochemical responses of *Pinus pinaster* trees to fire-induced trunk girdling and crown scorch: secondary metabolites and pigments as needle chemical indicators. J. Chem. Ecol. **28**: 687–700. doi:10.1023/A:1015276423880. PMID:12035919.

Anderson, H.E. 1969. Heat transfer and fire spread. USDA For. Serv. Res. Pap. INT-69.

Banavar, J.R., Damuth, J., Maritan, A., and Rinaldo, A. 2002. Supply-demand balance and metabolic scaling. Proc. Natl. Acad. Sci. U.S.A. **99**: 10506–10509. doi:10.1073/pnas.162216899. PMID:12149461.

Brown, A.A., and Davis, K.P. 1973. Forest fire: control and use. 2nd ed. McGraw-Hill Book Company, New York.

Brown, J.K., and DeByle, N.V. 1987. Fire damage, mortality, and suckering in aspen. Can. J. For. Res. **17**: 1100–1109. doi:10.1139/x87-168.

© 2008 NRC Canada

Burrows, N.D. 2001. Flame residence times and rates of weight loss of eucalypt forest fuel particles. Int. J. Wildland Fire, **10**: 137–143. doi:10.1071/WF01005.

Butler, B.W., Cohen, J., Latham, D.J., Schuette, R.D., Sopko, P., Shannon, K.S., Jimenez, D., and Bradshaw, L.S. 2004. Measurements of radiant emissive power and temperatures in crown fires. Can. J. For. Res. **34**: 1577–1587. doi:10.1139/x04-060.

Campbell, G.S., Jungbauer, J.D., Jr., Bristow, K.L., and Hungerford, R.D. 1995. Soil temperature and water content beneath a surface fire. Soil Sci. **159**: 363–374. doi:10.1097/00010694-199506000-00001.

Dickinson, M.B., and Johnson, E.A. 2004. Temperature-dependent rate models of vascular cambium cell mortality. Can. J. For. Res. **34**: 546–559. doi:10.1139/x03-223.

Dreyer, O., and Puzio, R. 2001. Allometric scaling in animals and plants. J. Math. Biol. **43**: 144–156. doi:10.1007/s002850170001. PMID:11570589.

Drysdale, D. 1999. An introduction to fire dynamics. 2nd ed. John Wiley & Sons, New York.

Ducrey, M., Duhoux, F., Huc, R., and Rigolot, E. 1996. The ecophysiological and growth responses of Aleppo pine (*Pinus halepensis*) to controlled heating applied to the base of the trunk. Can. J. For. Res. **26**: 1366–1374. doi:10.1139/x26-152.

Falster, D.S., Warton, D.I., and Wright, I.J. 2003. (S)MATR: standardised major axis tests and routines. Version 1.0. Available from www.bio.mq.edu.au/ecology/SMATR [accessed 2006].

Fay, J.A. 1994. Introduction to fluid mechanics. MIT Press, Cambridge, Mass.

Gill, A.M. 1995. Stems and fires. *In* Plant stems: physiology and functional morphology. *Edited by* B.L. Gartner. Academic Press, New York. pp. 323–342.

Gill, A.M., and Ashton, D.H. 1968. Role of bark type in relative tolerance to fire of three central Victorian eucalypts. Aust. J. Bot. **16**: 491–498. doi:10.1071/BT9680491.

Gill, A.M., Cheney, N.P., Walker, J., and Tunstall, B.R. 1986. Bark losses from two eucalypt species following fires of different intensities. Aust. For. Res. **16**: 1–7.

Gower, S.T., and Vogel, J.G. 1997. BOREAS TE-06 allometry data. Oak Ridge National Laboratory Distributed Active Archive Center, Oak Ridge, Tenn. Available from www-eosdis.ornl.gov/BOREAS/boreas_home_page.html [accessed 2006].

Gutsell, S.L., and Johnson, E.A. 1996. How fire scars are formed: coupling a disturbance process to its ecological effect. Can. J. For. Res. **26**: 166–174. doi:10.1139/x26-020.

Hall, R.J., Davidson, D.P., and Peddle, D.R. 2003. Ground and remote estimation of leaf area index in Rocky Mountain forest stands, Kananaskis, Alberta. Can. J. Remote Sens. **29**: 411–427.

Hartford, R.H., and Frandsen, W.H. 1992. When it's hot, it's hot… or maybe it's not! (Surface flaming may not portend extensive soil heating.) Int. J. Wildland Fire, **2**: 139–144. doi:10.1071/WF9920139.

Harmon, M.E. 1984. Survival of trees after low-intensity surface fires in Great Smoky Mountains National Park. Ecology, **65**: 796–802. doi:10.2307/1938052.

Harper, J.L. 1977. Population biology of plants. Academic Press, New York.

Hély, C., Flannigan, M., and Bergeron, Y. 2003. Modeling tree mortality following wildfire in the southeastern Canadian mixed-wood boreal forest. For. Sci. **49**: 566–576.

Hilpert, R. 1933. Wärmeabgabe von geheizten drähten und rohren im luftstrom. Forsch. Geb. Ingenieurwes. **4**: 215–224. doi:10.1007/BF02719754.

Huang, S. 1994. Ecologically based individual tree volume estimation for major Alberta tree species.1. Individual tree volume estimation procedures for Alberta: methods of formulation and statistical foundations. Alberta Environmental Protection, Land and Forest Services, Forest Management Division, Edmonton, Alta.

Incropera, F.P., DeWitt, D.P., Bergman, T.L., and Lavine, A.S. 2006. Fundamentals of heat and mass transfer. 6th ed. John Wiley & Sons, Inc., New York.

Johnson, E.A. 1992. Fire and vegetation dynamics: studies from the North American boreal forest. Cambridge University Press, New York.

Jones, J.L., Webb, B.W., Jimenez, D., Reardon, J., and Butler, B. 2004. Development of an advanced one-dimensional stem heating model for application in surface fires. Can. J. For. Res. **34**: 20–30. doi:10.1139/x03-187.

Martin, R.E. 1963. Thermal properties of bark. For. Prod. J. **13**: 419–426.

Matthews, S. 2006. A process-based model of fine fuel moisture. Int. J. Wildland Fire, **15**: 155–168. doi:10.1071/WF05063.

Mell, W., Jenkins, M.A., Gould, J., and Cheney, P. 2007. A physics-based approach to modeling grassland fires. Int. J. Wildland Fire, **16**: 1–22. doi:10.1071/WF06002.

Mercer, G.N., and Weber, R.O. 1994. Plumes above line fires in a crow wind. Int. J. Wildland Fire, **4**: 201–207. doi:10.1071/WF9940201.

Mercer, G.N., and Weber, R.O. 2001. Fire plumes. *In* Forest fires: behavior and ecological effects. *Edited by* E.A. Johnson and K. Miyanishi. Academic Press, New York. pp. 437–475.

Michaletz, S.T., and Johnson, E.A. 2006*a*. A heat transfer model of crown scorch in forest fires. Can. J. For. Res. **36**: 2839–2851. doi:10.1139/X06-158.

Michaletz, S.T., and Johnson, E.A. 2006*b*. Foliage influences forced convection heat transfer in conifer branches and buds. New Phytol. **170**: 87–98. doi:10.1111/j.1469-8137.2006.01661.x. PMID:16539606.

Millikin, D.E. 1955. Determination of bark volumes and fuel properties. Pulp Paper Mag. Can. **56**: 106–108.

Minore, D. 1979. Comparative autecological characteristics of northwestern tree species — a literature review. USDA For. Ser. Gen. Tech. Rep. PNW-87.

Miyanishi, K. 2001. Duff consumption. *In* Forest fires: behavior and ecological effects. Academic Press, New York. pp. 437–475.

Nelson, R.M., Jr. 2003. Reaction times and burning rates for wind tunnel headfires. Int. J. Wildland Fire, **12**: 195–211. doi:10.1071/WF02041.

Newnham, R.M. 1992. Variable-form taper functions for four Alberta tree species. Can. J. For. Res. **22**: 210–233. doi:10.1139/x92-028.

Niklas, K.J., and Spatz, H.-C. 2004. Growth and hydraulic (not mechanical) constraints govern the scaling of tree height and mass. Proc. Natl. Acad. Sci. U.S.A. **101**: 15 661 – 15 663. doi:10.1073/pnas.0405857101. PMID:15505224.

Parker, T.J., Clancy, K.M., and Mathiasen, R.L. 2006. Interactions among fire, insects and pathogens in coniferous forests of the interior western United States and Canada. Ag. For. Entomol. **8**: 167–189. doi:10.1111/j.1461-9563.2006.00305.x.

Patterson, M.R. 1992. A mass transfer explanation of metabolic scaling relations in some aquatic invertebrates and algae. Science (Washington, D.C.), **255**: 1421–1423. doi:10.1126/science.255.5050.1421. PMID:17801232.

Peng, C. 1999. Nonlinear height-diameter models for nine boreal forest tree species in Ontario. For. Res. Rep. 155. Ontario Forest Research Institute, Ontario Ministry of Natural Resources, Sault Ste. Marie, Ont.

© 2008 NRC Canada

Peterson, D.L., and Arbaugh, M.J. 1986. Postfire survival in Douglas-fir and lodgepole pine: comparing the effects of crown and bole damage. Can. J. For. Res. **16**: 1175–1179. doi:10.1139/x86-209.

Peterson, D.L., and Arbaugh, M.J. 1989. Estimating postfire survival of Douglas-fir in the Cascade Range. Can. J. For. Res. **19**: 530–533. doi:10.1139/x89-084.

Raupach, M.R. 1990. Similarity analysis of the interaction of bushfire plumes with ambient winds. Math. Comput. Model. **13**: 113–121. doi:10.1016/0895-7177(90)90105-V.

Rego, F., and Rigolot, E. 1990. Heat transfer through bark — a simple predictive model. *In* Fire in ecosystem dynamics. SPB Academic Publishing, The Hague, the Netherlands. pp. 157–161.

Rich, P.M., and Fournier, R.A. 1997. BOREAS TE-23 map plot data. Oak Ridge National Laboratory Distributed Active Archive Center, Oak Ridge, Tenn. Available online from www-eosdis.ornl.gov/BOREAS/boreas_home_page.html [accessed 2006].

Rosenberg, B., Kemeny, G., Switzer, R.C., and Hamilton, T.C. 1971. Quantitative evidence for protein denaturation as the cause of thermal death. Nature (London), **232**: 471–473. doi:10.1038/232471a0. PMID:4937206.

Ryan, K.C., and Frandsen, W.H. 1991. Basal injury from smoldering fires in mature *Pinus ponderosa* Laws. Int. J. Wildland Fire, **1**: 107–118. doi:10.1071/WF9910107.

Ryan, K.C., and Reinhardt, E.D. 1988. Predicting postfire mortality of seven western conifers. Can. J. For. Res. **18**: 1291–1297. doi:10.1139/x88-199.

Ryan, K.C., Peterson, D.L., and Reinhardt, E.D. 1988. Modeling long-term fire-caused mortality of Douglas-fir. For. Sci. **34**: 190–199.

Shinozaki, K., Yoda, K., Hozumi, K., and Kira, T. 1964. A quantitative analysis of plant form: pipe model theory. I. Basic analysis. Jpn. J. Ecol. **14**: 97–105.

Sokal, R.R., and Rohlf, F.J. 1995. Biometry: the principles and practice of statistics in biological research. 3rd ed. W.H. Freeman and Co., New York.

Spalt, K.W., and Reifsnyder, W.E. 1962. Bark characteristics and fire resistance: a literature survey. USDA For. Serv. Occas. Pap. 193.

Starker, T.J. 1934. Fire resistance in the forest. J. For. **33**: 595–598.

Swezy, D.M., and Agee, J.K. 1991. Prescribed fire effects on fine root and tree mortality in oldgrowth ponderosa pine. Can. J. For. Res. **21**: 626–634. doi:10.1139/x91-086.

Taylor, S.W., Wotton, B.M., Alexander, M.E., and Dalrymple, G.N. 2004. Variation in wind and crown fire behaviour in a northern jack pine – black spruce forest. Can. J. For. Res. **34**: 1561–1576. doi:10.1139/x04-116.

Tunstall, B.R., Walker, J., and Gill, A.M. 1976. Temperature distribution around synthetic trees during grass fires. For. Sci. **22**: 269–276.

Van Wagner, C.E. 1973. Height of crown scorch in forest fires. Can. J. For. Res. **3**: 373–378. doi:10.1139/x73-055.

Van Wagner, C.E. 1977. Conditions for the start and spread of crown fire. Can. J. For. Res. **7**: 23–34. doi:10.1139/x77-004.

Vargaftik, N.B. 1975. Tables of thermophysical properties of liquids and gases. 2nd ed. Hemisphere Publishing, New York.

Viney, N.R. 1991. A review of fine fuel moisture modeling. Int. J. Wildland Fire, **1**: 215–234. doi:10.1071/WF9910215.

Weber, R.O., Gill, A.M., Lyons, P.R.A., Moore, P.H.R., Bradstock, R.A., and Mercer, G.N. 1995. Modelling wildland fire temperatures. CALMScience, **Suppl. 4**: 23–26.

West, G.B., Brown, J.H., and Enquist, B.J. 1999. A general model for the structure and allometry of plant vascular systems. Nature (London), **400**: 664–667. doi:10.1038/23251.

White, J. 1979. The plant as a metapopulation. Annu. Rev. Ecol. Syst. **10**: 109–145. doi:10.1146/annurev.es.10.110179.000545.

Yuan, L.M., and Cox, G. 1996. An experimental study of some line fires. Fire Saf. J. **27**: 123–139. doi:10.1016/S0379-7112(96)00047-1.

Wyant, J.G., Omi, P.N., and Laven, R.D. 1986. Fire induced tree mortality in a Colorado ponderosa pine/Douglas-fir stand. For. Sci. **32**: 49–59.

Appendices

Appendices A and B appear on the following pages.

© 2008 NRC Canada

Appendix A

Table A1. List of papers published between 1980 and 2007 that contain at least one unique logistic regression model of postfire tree mortality.

Source	Species	Location	Covariates
Bevins (1980)	*Pseudotsuga menziesii*	West-central Montana	Crown scorch height, diameter at breast height
Peterson and Arbaugh (1986)	*Pinus contorta*, *P. menziesii*	Idaho, Montana, Wyoming	Basal scorch, crown scorch volume, insect damage
Brown and DeByle (1987)	*Populus tremuloides*	Idaho, Wyoming	Bark char circumference, bark char height (mean), diameter at breast height
Ryan and Reinhardt (1988)	*Abies lasiocarpa*, *Larix occidentalis*, *Picea engelmannii*, *P. contorta*, *P. menziesii*, *Thuja plicata*, *Tsuga heterophylla*	Idaho, Montana, Oregon, Washington	Bark thickness, crown scorch volume
Ryan et al. (1988)	*P. menziesii*	Western Montana	Cambium condition, crown scorch volume, diameter at breast height, foliage scorch height, season
Peterson and Arbaugh (1989)	*P. menziesii*	Oregon, Washington	Bark char depth, bark thickness, cambium condition, crown scorch volume, site
Rebertus et al. (1989)	*Quercus lae*vis	Southern Florida	Diameter at breast height, diameter at breast height of three nearest *Pinus palustris* trees, distance to three nearest *Pinus palustris* trees
Saveland and Neuenschwander (1990)	*Pinus ponderosa*	Northern Idaho	Crown scorch height, diameter at breast height
Finney and Martin (1993)	*Sequoia sempervirens*	Northwestern California	Crown scorch height, crown scorch volume, diameter at breast height, flame length, fuel consumption
Harrington (1993)	*P. ponderosa*	Southwestern Colorado	Crown scorch length, diameter at breast height, season
Regelbrugge and Conrad (1993)	*Caloccedrus decurrens*, *P. ponderosa*, *Quercus chrysolepis*, *Quercus kelloggii*	Central Sierra Nevada California	Bark char height (maximum), diameter at breast height
Regelbrugge and Smith (1994)	*Acer rubrum*, *Amelanchier* spp., *Carya glabra*, *Nyssa sylvatica*, *Quercus coccinea*, *Quercus prinus*, *Quercus rubra*, *Quercus velutina*	Virginia	Bark char height (maximum), diameter at breast height
Pausas (1997)	*Quercus suber*	Northeastern Spain	Bark thickness, diameter at breast height
Linder et al. (1998)	*Picea abies*, *Pinus sylvestris*	Northern Sweden	Diameter at breast height
Mutch and Parsons (1998)	*Abies concolor*, *Pinus lambertiana*	Southern Sierra Nevada California	Crown scorch volume, diameter at breast height
Guinto et al. (1999)	*Corymbia intermedia*, *Eucalyptus microcorys*, *Eucalyptus pilularis*, *Eucalyptus resinifera*, *Lophostemon confertus*, *Syncarpia glomulifera*	Australia	Diameter at breast height
Williams et al. (1999)	Unidentified spp.	Northern Australia	Diameter at breast height, fire regime, functional type
Gibbons et al. (2000)	Unidentified *Eucalyptus* spp.	Southeastern Australia	Aspect, basal area, silvicultural system
Higgins et al. (2000)	76 unidentified spp.	South Africa	Fireline intensity, tree height
Borchert et al. (2002)	*Pinus coulteri*, *Pinus sabiniana*	Central California	Bark char height (max.), crown scorch volume
Stephens and Finney (2002)	*A. concolor*, *Calocedrus decurrens*, *P. lambertiana*, *P. ponderosa*, *Sequoiadendron giganteum*	Southern Sierra Nevada California	Crown scorch height, crown scorch volume, diameter at breast height, fuel consumption
Barlow et al. (2003)	Amazonian forest spp.	Central Brazil	Bark char class, diameter at breast height, presence of buttresses
Beverly and Martell (2003)	*Pinus strobus*	Northwestern Ontario	Diameter at breast height, stem blackening height
Hély et al. (2003)	*Picea mariana*, *Pinus banksiana*, *P. tremuloides*	Northwestern Québec	Bark char height (max.), bark char height (mean), bark char height (min.), diameter at breast height, tree height
Kelsey and Joseph (2003)	*P. ponderosa*	Oregon	Ethanol concentration, water content
McHugh and Kolb (2003)	*P. ponderosa*	Northern Arizona	Bole char severity, crown consumption, crown scorch volume
McHugh et al. (2003)	*P. ponderosa*	Northern Arizona	Diameter at breast height, insect damage
van Mantgem et al. (2003)	*A. concolor*	California	Crown scorch volume, radial growth rate
Outcalt and Wade (2004)	*Pinus elliottii*, *Pinus paulstris*	Northwestern Florida	Diameter at breast height, percent bole char, percent crown death

© 2008 NRC Canada

Table A1 (*concluded*).

Source	Species	Location	Covariates
Rigolot (2004)	*Pinus halepensis*, *Pinus pinea*	Southeastern France	Bark char depth, crown scorch volume, diameter at breast height
van Mantgem and Schwartz (2004)	*P. ponderosa*	Central Sierra Nevada, California	Bark thickness, crown scorch class, stem scorch height
Dey and Hartman (2005)	*Carya* spp., *Cornus florida*, *Fraxinus americana*, *N. sylvatica*, *Pinus echinata*, *Quercus alba*, *Q. coccinea*, *Quercus marilandica*, *Quercus muehlenbergii*, *Quercus stellata*, *Q. velutina*	Missouri	Basal diameter, height
Raymond and Peterson (2005)	*P. menziesii*	Southwestern Oregon	Diameter at breast height, crown scorch height, number of dead cambium samples, percent volume crown scorch
Fensham and Fairfax (2006)	*Eucalyptus tereticornis*	Eastern Australia	lignotuber area, maximum temperature class
Franklin et al. (2006)	*A. concolor*, *C. decurrens*, *P. coulteri*, *Pinus jeffreyi*, *P. ponderosa*, *Quercus agrifolia*, *Q. chrysolepis*, *Q. kelloggii*	Southern Califronia	Diameter at breast height, species group
Keyser et al. (2006)	*P. ponderosa*	South Dakota	Diameter at breast height, bark thickness, percent bole char, percent crown length scorched
Kobziar et al. (2006)	*A. concolor*, *C. decurrens*, *Lithocarpus densiflorus*, *P. ponderosa*, *P. menziesii*, *Q. kelloggii*	California	Bole char severity rating, diameter at breast height, height, percent canopy closure, percent duff consumption, total crown damage
Perrakis and Agee (2006)	*P. ponderosa*	Southern Oregon	Diameter at breast height, fire treatment, Keen's crown vigor class
Schwilk et al. (2006)	*A. concolor*, *Abies magnifica*, *P. lambertiana*, *P. jeffreyi*, *P. ponderosa*	California	Bole char height, crown scorch height
Sieg et al. (2006)	*P. ponderosa*	Arizona, Colorado, Montana, South Dakota	Beetle presence, crown consumed volume, crown scorch volume, diameter at breast height, minimum bole scorch height, ground scorch severity, percent basal circumference scorched
Thies et al. (2006)	*P. ponderosa*	Eastern Oregon	Basal char, bole scorch proportion, bud kill proportion, foliage scorch proportion, live crown proportion
Hood and Bentz (2007)	*P. menziesii*	Montana, Wyoming	Beetle presence, crown scorch volume, cambium-kill rating, diameter at breast height
Hood et al. (2007)	*A. concolor*, *A. magnifica*, *C. decurrens*, *P. jeffreyi*, *P. ponderosa*	California	Beetle presence, diameter at breast height, cambium kill rating, percent crown length killed
Ritchie et al. (2007)	*P. ponderosa*	Northern California	Diameter at breast height, distance from stand boundary, disturbance history (treatment), structural diversity
Rodríguez-Trejo et al. (2007)	*Pinus hartwegii*	Central Mexico	Diameter at breast height, intensity class, season, stand density
Sidoroff et al. (2007)	*P. sylvestris*	Southern Finland	Charred stem ratio, diameter at breast height, bark thickness

© 2008 NRC Canada

References

Barlow, J., Lagan, B.O., and Peres, C.A. 2003. Morphological correlates of fire-induced tree mortality in a central Amazonian forest. J. Trop. Ecol. **19**: 291–299. doi:10.1017/S0266467403003328.

Beverly, J.L., and Martell, D.L. 2003. Modeling *Pinus strobus* mortality following prescribed fire in Quetico Provincial Park, northwestern Ontario. Can. J. For. Res. **33**: 740–751. doi:10.1139/x02-209.

Bevins, D.D. 1980. Estimating survival and salvage potential of fire-scarred Douglas-fir. USDA For. Ser. Res. Note, INT-287.

Borchert, M., Schreiner, D., Knowd, T., and Plumb, T. 2002. Predicting postfire survival in coulter pine (*Pinus coulteri*) and gray pine (*Pinus sabiniana*) after wildfire in central California. West. J. Appl. For. **17**: 134–138.

Brown, J.K., and DeByle, N.V. 1987. Fire damage, mortality, and suckering in aspen. Can. J. For. Res. **17**: 1100–1109. doi:10.1139/x87-168.

Dey, D.C., and Hartman, G. 2005. Returning fire to Ozark Highland forest ecosystems: effects on advance regeneration. For. Ecol. Manage. **217**: 37–53. doi:10.1016/j.foreco.2005.05.002.

Fensham, R.J., and Fairfax, R.J. 2006. Can burning restrict eucalypt invasion on grassy balds? Austral Ecol. **31**: 317–325. doi:10.1111/j.1442-9993.2006.01560.x.

Finney, M.A., and Martin, R.E. 1993. Modeling effects of prescribed fire on young-growth coast redwood trees. Can. J. For. Res. **23**: 1125–1135. doi:10.1139/x93-143.

Franklin, J., Spears-Lebrun, L.A., Deutschman, D.H., and Marsden, K. 2006. Impact of a high-intensity fire on mixed evergreen and mixed conifer forests in the Peninsular Ranges of southern California, USA. For. Ecol. Manage. **235**: 18–29. doi:10.1016/j.foreco.2006.07.023.

Gibbons, P., Lindenmayer, D.B., Barry, S.C., and Tanton, M.T. 2000. The effects of slash burning on the mortality and collapse of trees retained on logged sites in south-eastern Australia. For. Ecol. Manage. **139**: 51–61. doi:10.1016/S0378-1127(99)00333-3.

Guinto, D.F., House, A.P.N., Xu, Z.H., and Saffigna, P.G. 1999. Impacts of repeated fuel reduction burning on tree growth, mortality and recruitment in mixed species eucalypt forests of south-east Queensland, Australia. For. Ecol. Manage. **115**: 13–27. doi:10.1016/S0378-1127(98)00434-4.

Harrington, M.G. 1993. Predicting *Pinus ponderosa* mortality from dormant season and growing season fire injury. Int. J. Wildland Fire, **3**: 65–72. doi:10.1071/WF9930065.

Hély, C., Flannigan, M., and Bergeron, Y. 2003. Modeling tree mortality following wildfire in the southeastern Canadian mixed-wood boreal forest. For. Sci. **49**: 566–576.

Higgins, S.I., Bond, W.J., and Trollope, W.S.W. 2000. Fire, resprouting and variability: a recipe for grass-tree coexistence in savanna. J. Ecol. **88**: 213–229. doi:10.1046/j.1365-2745.2000.00435.x.

Hood, S.M., and Bentz, B. 2007. Predicting post-fire Douglas-fir beetle attacks and tree mortality in the Northern Rocky Mountains. Can. J. For. Res. **37**: 1058–1069. doi:10.1139/X06-313.

Hood, S.M., Smith, S.L., and Cluck, D.R. 2007. Delayed conifer tree mortality following fire in California. USDA For. Ser. Gen. Tech. Rep. PSW-GTR-203.

Kelsey, R.G., and Joseph, D.R. 2003. Ethanol in ponderosa pine as an indicator of physiological injury from fire and its relationship to secondary beetles. Can. J. For. Res. **33**: 870–884. doi:10.1139/x03-007.

Keyser, T.L., Smith, F.W., Lentile, L.B., and Shepperd, W.D. 2006. Modeling postfire mortality of ponderosa pine following a mixed-severity wildfire in the Black Hills: the role of tree morphology and direct fire effects. For. Sci. **52**: 530–539.

Kobziar, L., Moghaddas, J., and Stephens, S.L. 2006. Tree mortality patterns following prescribed fires in a mixed conifer forest. Can. J. For. Res. **36**: 3222–3238. doi:10.1139/X06-183.

Linder, P., Jonsson, P., and Niklasson, M. 1998. Tree mortality after prescribed burning in an old-growth Scots pine forest in northern Sweden. Silva Fenn. **32**: 339–349.

McHugh, C.W., and Kolb, T.E. 2003. Ponderosa pine mortality following fire in northern Arizona. Int. J. Wildland Fire, **12**: 7–22. doi:10.1071/WF02054.

McHugh, C.W., Kolb, T.E., and Wilson, J.L. 2003. Bark beetle attacks on ponderosa pine following fire in northern Arizona. Environ. Entomol. **32**: 510–522.

Mutch, L.S., and Parsons, D.J. 1998. Mixed conifer forest mortality and establishment before and after prescribed fire in Sequoia National Park, California. For. Sci. **4**: 341–355.

Outcalt, K.W., and Wade, D.D. 2004. Fuels management reduces tree mortality from wildfires in southeastern United States. South. J. Appl. For. **28**: 28–34.

Pausas, J.G. 1997. Resprouting of *Quercus suber* in NE Spain after fire. J. Veg. Sci. **8**: 703–706. doi:10.2307/3237375.

Perrakis, D.D.B., and Agee, J.K. 2006. Seasonal fire effects on mixed-conifer forest structure and ponderosa pine resin properties. Can. J. For. Res. **36**: 238–254. doi:10.1139/x05-212.

Peterson, D.L., and Arbaugh, M.J. 1986. Postfire survival in Douglas-fir and lodgepole pine: comparing the effects of crown and bole damage. Can. J. For. Res. **16**: 1175–1179. doi:10.1139/x86-209.

Peterson, D.L., and Arbaugh, M.J. 1989. Estimating postfire survival of Douglas-fir in the Cascade Range. Can. J. For. Res. **19**: 530–533. doi:10.1139/x89-084.

Raymond, C.L., and Peterson, D.L. 2005. Fuel treatments alter the effects of wildfire in a mixed-evergreen forest, Oregon, USA. Can. J. For. Res. **35**: 2981–2995. doi:10.1139/x05-206.

Rebertus, A.J., Williamson, G.B., and Moser, E.B. 1989. Longleaf pine pyrogenicity and turkey oak mortality in Florida xeric sandhills. Ecology, **70**: 60–70. doi:10.2307/1938412.

Regelbrugge, J.C., and Conrad, S.G. 1993. Modeling tree mortality following wildfire in *Pinus ponderosa* forests in the central Sierra-Nevada of California. Int. J. Wildland Fire, **3**: 139–148. doi:10.1071/WF9930139.

Regelbrugge, J.C., and Smith, D.W. 1994. Postfire tree mortality in relation to wildfire severity in mixed oak forests in the Blue Ridge of Virginia. North. J. Appl. For. **11**: 90–97.

Rigolot, E. 2004. Predicting postfire mortality of *Pinus halpensis* Mill., and *Pinus pinea* L. Plant Ecol. **171**: 139–151. doi:10.1023/B:VEGE.0000029382.59284.71.

Ritchie, M.W., Skinner, C.N., and Hamilton, T.A. 2007. Probability of tree survival after wildfire in an interior pine forest of northern California: effects of thinning and prescribed fire. For. Ecol. Manage. **247**: 200–208. doi:10.1016/j.foreco.2007.04.044.

Rodríguez-Trejo, D.A., Castro-Solis, U.B., Zepeda-Bautista, M., and Carr, R.J. 2007. First year survival of *Pinus hartwegii* following prescribed burns at different intensities and different seasons in central Mexico. Int. J. For. Res. **16**: 54–62.

Ryan, K.C., Peterson, D.L., and Reinhardt, E.D. 1988. Modeling long-term fire-caused mortality of Douglas-fir. For. Sci. **34**: 190–199.

Ryan, K.C., and Reinhardt, E.D. 1988. Predicting postfire mortality of seven western conifers. Can. J. For. Res. **18**: 1291–1297. doi:10.1139/x88-199.

Saveland, J.M., and Neuenschwander, L.F. 1990. A signal detection framework to evaluate models of tree mortality following fire damage. For. Sci. **36**: 66–76.

Schwilk, D.W., Knapp, E.E., Ferrenberg, S.M., Keeley, J.E., and Caprio, A.C. 2006. Tree mortality from fire and bark beetles fol-

© 2008 NRC Canada

lowing early and late season prescribed fires in a Sierra Nevada mixed-conifer forest. For. Ecol. Manage. **232**: 36–45. doi:10.1016/j.foreco.2006.05.036.

Sidoroff, K., Kuuluvainen, T., Tanskanen, H., and Vanha-Majamaa, I. 2007. Tree mortality after low-instensity prescribed fires in managed *Pinus sylvestris* stands in southern Finland. Scand. J. For. Res. **22**: 2–12. doi:10.1080/02827580500365935.

Sieg, C.H., McMillin, J.D., Fowler, J.F., Allen, K.K., Negron, J.F., Wadleigh, L.L., Anhold, J.A., and Gibson, K.E. 2006. Best predictors for postfire mortality of ponderosa pine trees in the intermountain west. For. Sci. **52**: 718–728.

Stephens, S.L., and Finney, M.A. 2002. Prescribed fire mortality of Sierra Nevada mixed conifer tree species: effects of crown damage and forest floor combustion. For. Ecol. Manage. **162**: 261–271. doi:10.1016/S0378-1127(01)00521-7.

Thies, W.G., Westlind, D.J., Loewen, M., and Brenner, G. 2006. Prediction of delayed mortality of fire-damaged ponderosa pine following prescribed fires in eastern Oregon, USA. Int. J. Wildland Fire, **15**: 19–29. doi:10.1071/WF05025.

van Mantgem, P., and Schwartz, M. 2004. An experimental demonstration of stem damage as a predictor of fire-caused mortality for ponderosa pine. Can. J. For. Res. **34**: 1343–1347. doi:10.1139/x04-001.

van Mantgem, P.J., Stephenson, N.L., Mutch, L.S., Johnson, V.G., Esperanza, A.M., and Parsons, D.J. 2003. Growth rate predicts mortality of *Abies concolor* in both burned and unburned stands. Can. J. For. Res. **33**: 1029–1038. doi:10.1139/x03-019.

Williams, R.J., Cook, G.D., Gill, A.M., and Moore, P.H.R. 1999. Fire regime, fire intensity and tree survival in a tropical savanna in northern Australia. Aust. J. Ecol. **24**: 50–59. doi:10.1046/j.1442-9993.1999.00946.x.

Appendix B. Parameter estimates used in model calculations

Table B1. Slopes (a) and intercepts (b) for eq. 19 relating bark thickness (x; cm) and bole diameter (D; cm; calculated from Huang 1994).

Species	a	b	R^2
Picea glauca	0.012	0.237	0.999
Pinus contorta var. *latifolia*	0.012	0.138	0.999
Populus tremuloides	0.036	0.042	0.998

Table B2. Functions used to calculate scaling exponents 1/exp F in bole taper eq. 21 (Newnham 1991).

Species	F
Picea glauca	$0.934 + 0.603X - 0.231\mathrm{DBH}/Z - 0.447/\sqrt{z} + 0.0170Z/z - 0.0656Z/\sqrt{z}$
Pinus banksiana, *Pinus contorta*	$0.772 + 0.959X - 0.0529(\mathrm{DBH}/Z)^2 - 0.364X^2\mathrm{DBH}/Z - 0.0630Z/\sqrt{z} + 0.000232\mathrm{DBH}(Z/z)$
Populus tremuloides	$0.214 + 0.0967X - 0.559X^3\mathrm{DBH}/Z + 0.0308/z + 0.0621(\mathrm{DBH}/Z)/z^2 - 0.0242Z/z$

Note: $X = [(Z-z)/(Z-1.30)]$. Nomenclature is as defined in Table 1.

Table B3. Normalization constants (B) and scaling exponents (n) for eq. 22 relating tree height Z (m) and diameter at breast height $D_{1.3}$ (cm; Peng 1999).

Species	B	n	R^2
Picea glauca	0.865	0.892	0.963
Pinus banksiana	1.307	0.835	0.958
Populus tremuloides	2.612	0.635	0.975

Table B4. Inverse thermal time constants ($hA/\rho cV$) (±SEM) for buds (used for eq. 13) and corresponding critical plume temperature T_c (±SEM; calculated from eq. 15, assuming T_a = 25 °C; Michaletz and Johnson 2006).

Species	N	Foliage	$\frac{hA}{\rho cV} \times 10^3 (\mathrm{s}^{-1})$	T_c (°C)
Picea glauca	600	Present	13.63±0.30	98.10±1.26
Pinus contorta	600	Present	8.95±0.22	124.59±1.37
Populus tremuloides	600	Absent	59.16±1.93	64.72±0.50

Note: Heat transfer coefficients (h) were calculated for foliated *P. glauca* and *P. contorta* buds and leafless *P. tremuloides* buds. Numerical values are presented according to the convention $hA/\rho cV \times 103$ (s^{-1}), where $hA/\rho cV = 13.63 \times 10^{-3} \pm 0.30 \times 10^{-3}\ \mathrm{s}^{-1} = 0.01363 \pm 0.00030\ \mathrm{s}^{-1}$. Nomenclature is as defined in Table 1.

Table B5. Normalization constants (B) and scaling exponents (n) for eq. 20 relating sapwood area (SA; cm^2) and bole diameter (D; cm).

Species	B	n (95% CI)	R^2
Picea glauca	1.030	1.64 (1.48–1.81)	0.853
Pinus contorta var. *latifolia*	0.281	2.14 (2.00–2.30)	0.916
Populus balsamifera, *Populus tremuloides*	0.154	2.29 (2.09–2.51)	0.823

Note: Log-transformed data from Hall et al. (2003) were fit using Model II reduced major axis regression (Sokal and Rohlf 1995).

References

Hall, R.J., Davidson, D.P., and Peddle, D.R. 2003. Ground and remote estimation of leaf area index in Rocky Mountain forest stands, Kananaskis, Alberta. Can. J. Remote Sens. **29**: 411–427.

Huang, S. 1994. Ecologically based individual tree volume estimation for major Alberta tree species. Report to Alberta Environmental Protection, Land and Forest Services, Forest Management Division, Edmonton, Alta.

Michaletz, S.T., and Johnson, E.A. 2006. A heat transfer model of crown scorch in forest fires. Can. J. For. Res. **36**: 2839–2851. doi:10.1139/X06-158.

Newnham, R.M. 1992. Variable-form taper functions for four Alberta tree species. Can. J. For. Res. **22**: 210–233. doi:10.1139/x92-028.

Peng, C. 1999. Nonlinear height-diameter models for nine boreal forest tree species in Ontario. For. Res. Rep. 155. Ontario Forest Research Institute, Ontario Ministry of Natural Resources, Sault Ste. Marie, Ont.

Sokal, R.R., and Rohlf, F.J. 1995. Biometry: the principles and practice of statistics in biological research. 3rd ed. W.H. Freeman and Co., New York.

© 2008 NRC Canada